

## RESEARCH ARTICLE

View Article Online  
View Journal | View IssueCite this: *Mater. Chem. Front.*,  
2017, 1, 507

## Fabrication of convex lens-shaped polymer particles by tuning the interfacial interaction†

Jiangping Xu, Yi Yang, Ke Wang, Yuqing Wu and Jintao Zhu\*

In this communication, we report a facile yet effective approach to fabricate polystyrene-*b*-poly(4-vinyl pyridine) (PS-*b*-P4VP) convex lens (CL)-like microparticles with hexagonally stacked cylindrical P4VP domains *via* three-dimensional confined assembly. Addition of a hydrogen bonding agent, 3-*n*-pentadecylphenol (PDP), not only changes the volume fraction of the P4VP domain, but also alters the interfacial interactions between the blocks and the surfactant. A neutral interface could be created by tuning the content of PDP, resulting in the formation of CL-like microparticles. Selective swelling and then deswelling of these particles offers us a convenient way to synthesize isoporous particles with tunable pore size, potentially useful in ultrafiltration with high selectivity.

Received 30th May 2016,  
Accepted 27th August 2016

DOI: 10.1039/c6qm00072j

rsc.li/frontiers-materials

Structured block copolymer (BCP) particles have attracted significant attention owing to their various applications in photonics,<sup>1,2</sup> sensing,<sup>3</sup> template synthesis,<sup>4–6</sup> and as catalytic substrates.<sup>7</sup> Confined assembly of BCPs in small droplets could be especially useful in fabricating particles with unconventional shapes, internal structures, and surface properties.<sup>8–14</sup> Under three-dimensional (3D) confinement, the microphase separation of BCPs gives access to unique shapes and structures, which could be tailored by changing the volume fraction of blocks, particle size, and interfacial interactions between each block and the surrounding medium.<sup>10,11,15,16</sup> Among these factors, the interfacial interaction is especially important due to the large surface area/volume ratio of the BCP particles.<sup>17,18</sup> Generally, the properties of the surfactants govern the interfacial interaction and thus can shape the morphology of the particles. Manipulation of the interfacial interaction between BCP blocks and the surrounding medium can be achieved by applying mixed surfactants, which have different affinities for each block of the BCP chain.<sup>17,19–24</sup>

Recently, shaped anisotropic particles have gained increasing interest due to their unique properties in optics<sup>24</sup> or cell internalization.<sup>25</sup> By precisely tailoring the interfacial interaction, anisotropic particles from BCPs can be readily obtained *via* an emulsion–solvent evaporation technique. This facile and scalable approach allows control over not only the particle internal structure, but also their overall shape. It is of great importance to control the morphology of BCP colloids by independently and selectively tailoring the interfacial properties at the desired

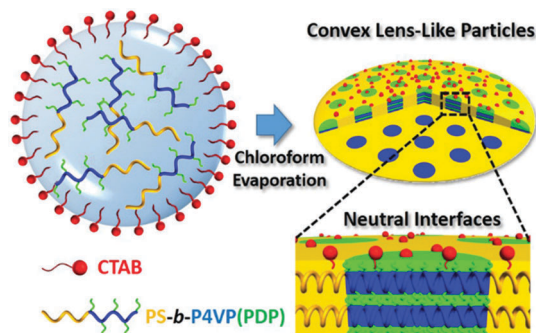
location along the interface. For example, mixtures of surfactants with different affinities to BCP blocks were introduced to control the shape and the internal structure of the particles.<sup>12,17,19,20</sup> Moreover, inorganic particles with different surface properties could also be applied as surfactants to tune the interfacial interactions and thus morphology of the particles.<sup>22–24,26</sup> Highly specific functional properties of BCP particles are achieved by simultaneously controlling shape anisotropy and the internal structure from nano- to micro-meter length scale. In particular, the convex lens (CL)-like particles<sup>19,20</sup> with hexagonally packed cylinders perpendicular to the long axis are of significant interest due to their potential application in concentrating light with enhanced near-field signals.<sup>24</sup> Generally, to fabricate such particles, two types of surfactants with different affinities were essential for creating a neutral interface for each block. To the best of our knowledge, these particles with a unique shape could not be obtained by using a single surfactant.

Under 3D confinement, the properties of the interface are mainly governed by the properties of surfactants. On the other hand, the properties of the BCP matrix also significantly affect the interfacial interaction. Herein, we report the manipulation of interfacial interaction by introducing a hydrogen-bonding agent (3-*n*-pentadecylphenol, PDP) into the polystyrene-*b*-poly(4-vinyl pyridine) (PS-*b*-P4VP) matrix. The affinities of the surfactants to BCP chains are tailored by varying the content of PDP, rather than altering the surfactants. Based on this strategy, a neutral interface can be easily generated and consequently the CL-like microparticles can be obtained by using a single surfactant (Scheme 1).

The asymmetric PS<sub>51K</sub>-*b*-P4VP<sub>18K</sub> (subscripts are the  $M_n$  of the blocks) was employed to fabricate BCP particles through an emulsion–solvent evaporation method by using cetyltrimethylammonium bromide (CTAB, 3 mg mL<sup>-1</sup>) as the emulsifier

Key Laboratory of Materials Chemistry for Energy Conversion and Storage,  
Ministry of Education, School of Chemistry and Chemical Engineering,  
Huazhong University of Science and Technology, Wuhan 430074, China.  
E-mail: jtzhu@mail.hust.edu.cn

† Electronic supplementary information (ESI) available: Experimental details and additional figures of the BCP particles. See DOI: 10.1039/c6qm00072j



**Scheme 1** Illustration showing the formation of convex lens-like particles by tailoring the interfacial interaction via an emulsion–solvent evaporation method. The P4VP(PDP) cylindrical domains pack hexagonally and are vertical to the long axis of the particles. These cylinders persist throughout the entire thickness of the particles.

(see experimental details in the ESI†). After evaporation of chloroform from the emulsion droplets, particles with P4VP discrete spherical domains (volume fraction of P4VP:  $f_{P4VP} = 24.4 \text{ vol}\%$ ) and PS on the particle surface are obtained (Fig. 1a), since CTAB selectively wets PS domains.<sup>12,17,24</sup> When the hydrogen bond assisted supramolecules  $PS_{51K}\text{-}b\text{-}P4VP_{18K}(\text{PDP})_x$  ( $x$  is the molar ratio of PDP to 4VP) are introduced to form the particles, the morphology of the particles changes significantly with the increase of  $x$  (Fig. 1b–f). The CL-like microparticles with hexagonally packed P4VP(PDP) cylindrical domains start to appear at  $x = 0.05$  and become the dominant morphology at  $x = 0.2$  (Fig. 1d). The tilted TEM images (Fig. S1, ESI†) indicate that the P4VP(PDP) cylinders persist throughout the entire thickness of the BCP particles. The SEM image (Fig. S2a and b, ESI†) confirms the CL-like shape of the particles, and the Voronoi diagram (Fig. S2c and d, ESI†) indicates that the cylindrical

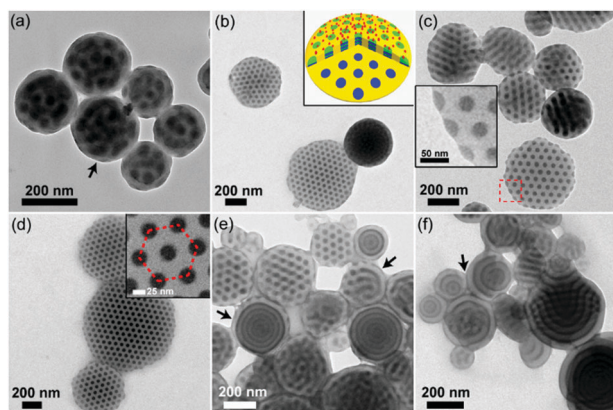


**Fig. 1** TEM images of  $PS_{51K}\text{-}b\text{-}P4VP_{18K}(\text{PDP})_x$  particles obtained by employing CTAB ( $3 \text{ mg mL}^{-1}$ ) as the surfactant. The content of PDP is (a)  $x = 0$ , (b)  $x = 0.05$ , (c)  $x = 0.10$ , (d)  $x = 0.20$ , (e)  $x = 0.60$ , and (f)  $x = 1.0$ , respectively. The arrow in (a) indicates that the outermost layer is PS. The inset in (b) is the cartoon showing the internal structures of the particles while the inset in (c) shows that both P4VP(PDP) and PS can locate on the interface. The inset in (d) shows the vertically and hexagonally stacked cylinders. The arrows in (e) and (f) indicate that the outermost layer is P4VP(PDP). The P4VP(PDP) domains are selectively stained by  $I_2$  vapor before TEM investigation.

P4VP(PDP) domains are well-oriented and highly ordered.<sup>24,27</sup> Both PS and P4VP(PDP) can locate on the surface of the CL-like particles (Fig. 1c), implying a neutral interface for both blocks. PDP has a long alkyl tail, which increases the affinity of the P4VP(PDP) domain to CTAB. Moreover, the hydrophilic phenol head of PDP increases the hydrophilicity of the P4VP(PDP) block. Therefore, P4VP(PDP) segments will migrate to the surface of the particles. This could lead to a balanced interfacial interaction between PS/P4VP(PDP) domains and the surrounding water. In this case, the BCPs will self-assemble into a morphology with low curvature boundary to minimize the entropic penalty associated with bending of the polymer chains. The surface energy varies at different positions on the particles, due to different packing structures of polymer chains at the lateral surface and the end surface of the particles (Scheme S1, ESI†), inducing the transformation of spherical particles into CL-like particles.<sup>26</sup> Additionally, the increase of PDP will enlarge the volume fraction of the P4VP domain ( $x = 0.2$ ,  $f_{P4VP(\text{PDP})} = 35.8 \text{ vol}\%$ ), resulting in morphological evolution from sphere to cylinder.<sup>15</sup> Consequently, CL-like particles with perfectly stacked cylinders are obtained by varying the properties of the BCP matrix, rather than changing the composition of surfactants. In previous studies, CL-like particles can only be obtained by employing two types of surfactants. Our results demonstrate that by carefully adding additives to tailor the properties of the BCP matrix, the CL-like particles can be readily obtained by using a single commercially available surfactant. A further increase of  $x$  results in the continuous increase of the affinity of P4VP(PDP) to CTAB and the volume fraction of the P4VP(PDP) domain, triggering the formation of onion-like particles with P4VP(PDP) on the surface (Fig. 1e and f). In this case, CTAB selectively wets P4VP(PDP) instead of PS domains.

In our previous report, we demonstrated the morphological transition of the  $PS_{51K}\text{-}b\text{-}P4VP_{18K}(\text{PDP})_x$  particles stabilized by poly(vinyl alcohol) (PVA).<sup>15</sup> Since PVA has almost the same affinities to PS and P4VP, it can generate a neutral interface for PS and P4VP segments. Consequently, both blocks can simultaneously locate on the surface of the particles. However, the addition of PDP will increase the attractive interaction between P4VP(PDP) and the surrounding water, as PDP has a hydrophilic phenol head. No CL-like particles can be obtained in that case since the interfaces are selective for P4VP(PDP) instead of being neutral to both blocks.

In a similar report by Kim *et al.*, they found that CL-like particles could not be formed by  $PS_{27K}\text{-}b\text{-}P4VP_{7K}(\text{PDP})_{0.2}$  in CTAB ( $5 \text{ mg mL}^{-1}$ ), although the volume fraction of P4VP(PDP) ( $f_{P4VP(\text{PDP})} = 29.1 \text{ vol}\%$ ) is located in the cylindrical regime.<sup>24</sup> Presumably, high concentrations of CTAB would retard the formation of CL-like particles. More CTAB will induce more P4VP(PDP) chains to the interface, resulting in the breaking of the neutral interface for both PS and P4VP(PDP). Thus, P4VP(PDP) will locate on the surface of the particles in this case. In order to prove this assumption, we fabricate  $PS_{51K}\text{-}b\text{-}P4VP_{18K}(\text{PDP})_{0.2}$  particles with CTAB of  $5 \text{ mg mL}^{-1}$  concentration. Indeed, no CL-like particles can be observed in this case (Fig. S3, ESI†).

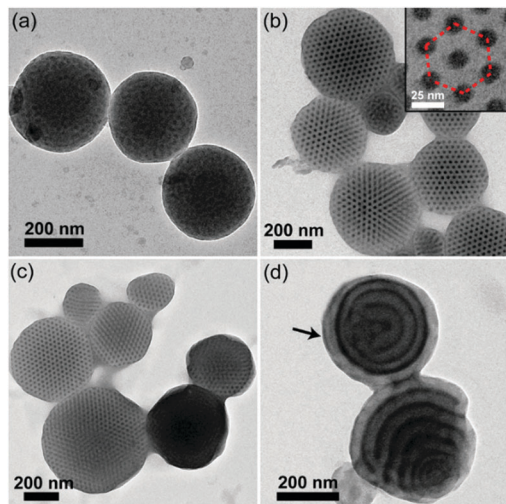


**Fig. 2** TEM images of the  $P4VP_{4.5K}\text{-}b\text{-}PS_{38K}\text{-}b\text{-}P4VP_{4.5K}(PDP)_x$  particles, where  $x$  equals (a) 0, (b) 0.25, (c) 0.50, and (d) 1.0. The inset in (b) shows the vertically and hexagonally stacked cylinders. The arrow in (d) indicates that the outermost layer of the particles is P4VP(PDP). The P4VP(PDP) domains are selectively stained by  $I_2$  vapor before TEM investigation.

In order to demonstrate the generality of our strategy, triblock copolymer-based supramolecules  $P4VP_{4.5K}\text{-}b\text{-}PS_{38K}\text{-}b\text{-}P4VP_{4.5K}(PDP)_x$  are employed to fabricate CL-like particles by using CTAB as a surfactant ( $3\text{ mg mL}^{-1}$ ). As shown in Fig. 2, CL-like particles can be observed at  $x = 0.25\text{--}0.50$ . Onion-like particles with P4VP(PDP) on the surface are obtained at  $x = 1.0$ . However, no CL-like particles can be observed if PVA was used as an emulsifier when  $x$  is increased from 0 to 1.0 (Fig. S4, ESI†). The results coincide with those of the  $PS_{51K}\text{-}b\text{-}P4VP_{18K}(PDP)_x$  system. We presume that the fraction of CTAB in the surfactant solution would play an important role in the formation of CL-like particles. Thus, mixed surfactants of CTAB and PVA with different weight ratios ( $w$ ) are employed for fabricating BCP particles. As shown in Fig. 3, when  $w = 1:9$ , no CL-like particles can be observed (Fig. 3a), whereas when  $w$  is higher than  $1:9$  (for instance,  $1:7$ ,  $1:5$ , and  $1:3$ ), CL-like particles are formed. A solvent-absorption annealing approach (details are given in the ESI†) can be applied to shape the morphology of the BCP particles after their formation.<sup>12,16,18,28</sup> The particles with a twisted cylindrical structure (Fig. 3a) are employed as the initial state during the annealing process. After removal of the mixed surfactants with  $w = 1:9$ , the particles are redispersed in mixed surfactants with  $w = 1:5$  or  $1:3$ . The spherical particles with twisted cylinders transform into CL-like particles after being annealed in chloroform for 8 h (Fig. S5, ESI†). The interfacial interaction between polymers and surfactants dominates the shape and the internal structure of the particles. Therefore, CL-like particles can be obtained through either of these two approaches, *e.g.*, an emulsion-solvent evaporation method or a solvent-absorption annealing method, provided the neutral interfacial interaction is established.<sup>12</sup>

The CL-like particles can be transformed into mesoporous particles (Fig. 4) since the P4VP(PDP) domains can be swelled and the PDP can be removed using a selective solvent.<sup>15,29</sup>

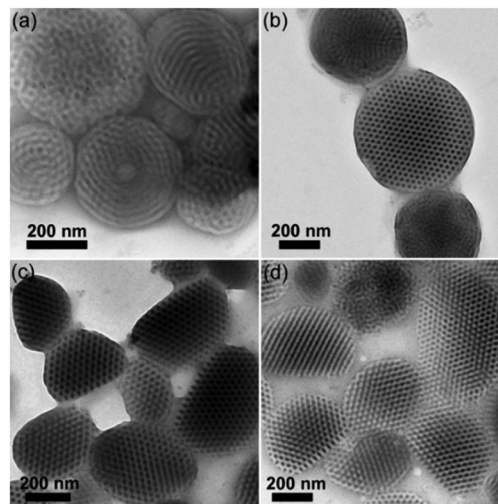


**Fig. 3** TEM images of the  $P4VP_{4.5K}\text{-}b\text{-}PS_{38K}\text{-}b\text{-}P4VP_{4.5K}(PDP)_x$  particles, where  $x$  equals 0.25. The PVA/CTAB mixed surfactants are used to fabricate the particles. The weight ratios ( $w$ ) of CTAB to PVA are (a)  $1:9$ , (b)  $1:7$ , (c)  $1:5$ , and (d)  $1:3$ , respectively. The P4VP(PDP) domains are selectively stained by  $I_2$  vapor before TEM investigation.

The pore size is dominated by two factors: (1) the size of P4VP(PDP) domains and (2) the swelling temperature. The diameters of P4VP(PDP) domains within the CL-like particles shown in Fig. 2c and Fig. 1d are  $14.0 \pm 0.5\text{ nm}$  and  $30.2 \pm 1.3\text{ nm}$ , respectively. After swelling at  $25\text{ }^\circ\text{C}$  for 24 h, the diameters of the pores turn out to be  $6.0 \pm 0.8\text{ nm}$  and  $16.0 \pm 2.0\text{ nm}$ , respectively (Fig. 4a and b). Heating will increase the stretching of P4VP chains in ethanol, inducing the enlargement of the pores. As shown in Fig. 4c and d, after swelling at  $60\text{ }^\circ\text{C}$  for 20 min, the diameters of the pores increase to  $15.5 \pm 1.0\text{ nm}$  and  $50.4 \pm 1.9\text{ nm}$ , even larger than the initial diameter of the P4VP(PDP) cylinder. Since heating will soften the PS matrix, the stretching of P4VP chains will expand the PS chains, leading to larger pores. A similar phenomenon has been reported in our previous study.<sup>16</sup> Interestingly, the size of the mesopores is nearly monodispersed. Thus, the strategy presented here can be used for preparing particles with isoporosity and tunable pore size, which could be potentially applied in ultrafiltration.<sup>30–33</sup>

The 3D confined assembly-disassembly strategy was recently developed to fabricate nano-objects with designable morphologies.<sup>9,12,34,35</sup> Here, the CL-like particles with hexagonally stacked P4VP(PDP) cylinders are employed for the disassembly process, and isolated nanofibers with monodispersed diameter are expected. The P4VP(PDP) domains are crosslinked by 1,4-diiodobutane (DIB) before dispersing the particles in chloroform to dissolve the PS matrix. However, only spherical particles with crosslinked P4VP cores are obtained after disassembly of the CL-like particles (Fig. 5). Inside the P4VP(PDP) domains, microphase separation between the P4VP chains and PDP chains occurs (Scheme 1).<sup>36</sup> Therefore, the crosslinking of 4VP by DIB is suppressed by the PDP sub-domains, leading to the incomplete crosslinking of the P4VP(PDP) cylinders. As a result, the disassembly process in chloroform will make the cylinders break up into small pieces, resulting in spherical particles



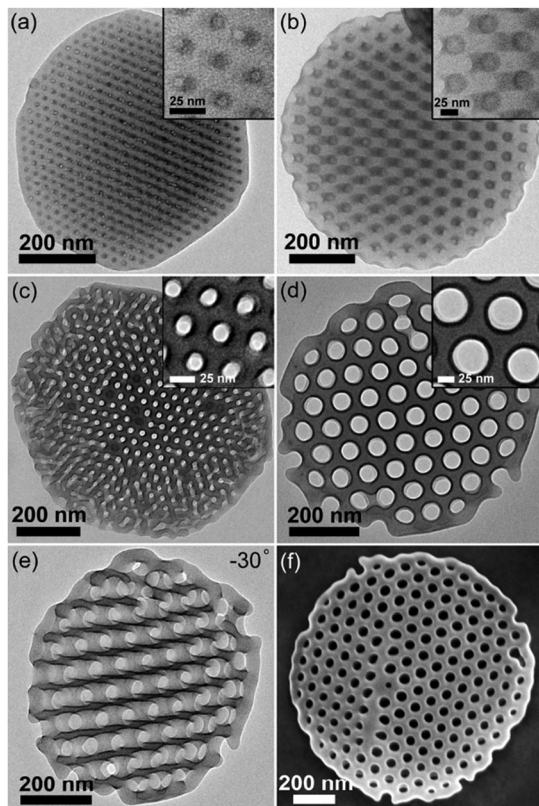


Fig. 4 TEM (a–e) and SEM (f) images of the porous CL-like particles obtained by ethanol swelling at different temperatures. (a) P4VP<sub>4.5K</sub>-b-PS<sub>38K</sub>-b-P4VP<sub>4.5K</sub>(PDP)<sub>0.25</sub>, 25 °C, (b) PS<sub>51K</sub>-b-P4VP<sub>18K</sub>(PDP)<sub>0.2</sub>, 25 °C, (c) P4VP<sub>4.5K</sub>-b-PS<sub>38K</sub>-b-P4VP<sub>4.5K</sub>(PDP)<sub>0.25</sub>, 60 °C, and (d) PS<sub>51K</sub>-b-P4VP<sub>18K</sub>(PDP)<sub>0.2</sub>, 60 °C. (e) Tilted TEM image of the particle shown in (d). (f) SEM image of the porous particle from PS<sub>51K</sub>-b-P4VP<sub>18K</sub>(PDP)<sub>0.2</sub> at 60 °C. The insets in (a–d) show the TEM images with a higher magnification. The pore diameters are (a)  $6.0 \pm 0.8$  nm, (b)  $16.0 \pm 2.0$  nm, (c)  $15.5 \pm 1.0$  nm, and (d)  $50.4 \pm 1.9$  nm, respectively. The P4VP domains are selectively stained by I<sub>2</sub> vapor before TEM investigation.

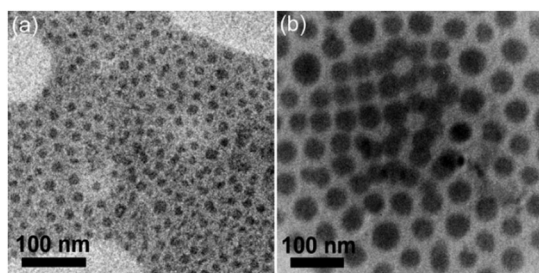


Fig. 5 TEM images of the spheres obtained by disassembling the CL-like particles after crosslinking P4VP(PDP) domains. The BCPs are (a) P4VP<sub>4.5K</sub>-b-PS<sub>38K</sub>-b-P4VP<sub>4.5K</sub>(PDP)<sub>0.25</sub>, and (b) PS<sub>51K</sub>-b-P4VP<sub>18K</sub>(PDP)<sub>0.2</sub>, respectively. Diameters of P4VP cores in the spheres are (a)  $15.1 \pm 1.8$  nm, and (b)  $38.3 \pm 4.6$  nm, respectively. The P4VP domains are selectively stained by I<sub>2</sub> vapor before TEM investigation.

instead of cylindrical nanofibers. In order to confirm this assumption, P4VP<sub>4.5K</sub>-b-PS<sub>27K</sub>-b-P4VP<sub>4.5K</sub> (without PDP,  $f_{P4VP} = 23.3$  vol%) was introduced to fabricate particles with cylindrical structures. After crosslinking by DIB and disassembling in chloroform,

nanofibers can be obtained (Fig. S6, ESI<sup>†</sup>). In this case, the P4VP domains are completely crosslinked and thus the internal structure can be preserved after disassembly.

## Conclusions

In summary, we have demonstrated a facile yet efficient approach to fabricate anisotropic CL-like particles with hexagonally stacked cylindrical domains by employing a single surfactant to construct a neutral interface for both blocks. Additives are introduced into the BCP matrix to tailor the interfacial interaction between the polymer chains and the surrounding medium. More interestingly, by selectively swelling the P4VP(PDP) domains, isoporous particles with uniform channels are obtained, which can be potentially applied in separation membranes with high selectivity.

## Acknowledgements

We gratefully acknowledge funding of this work provided by the National Basic Research Program of China (973 Program, 2012CB821500), National Natural Science Foundation of China (51473059 and 51525302), and Natural Science Foundation of Hubei Scientific Committee (2015BHE001). We also thank the HUST Analytical and Testing Center for allowing us to use its facilities.

## Notes and references

- 1 S.-H. Kim, S. Y. Lee, S.-M. Yang and G.-R. Yi, *NPG Asia Mater.*, 2011, **3**, 25–33.
- 2 M. Bockstaller, R. Kolb and E. L. Thomas, *Adv. Mater.*, 2001, **13**, 1783–1786.
- 3 A. Setaro, S. Lettieri, P. Maddalena and L. De Stefano, *Appl. Phys. Lett.*, 2007, **91**, 051921.
- 4 M. P. Kim, D. J. Kang, D.-W. Jung, A. G. Kannan, K.-H. Kim, K. H. Ku, S. G. Jang, W.-S. Chae, G.-R. Yi and B. J. Kim, *ACS Nano*, 2012, **6**, 2750–2757.
- 5 L. A. Connal, N. A. Lynd, M. J. Robb, K. A. See, S. G. Jang, J. M. Spruell and C. J. Hawker, *Chem. Mater.*, 2012, **24**, 4036–4042.
- 6 K. H. Ku, M. P. Kim, K. Paek, J. M. Shin, S. Chung, S. G. Jang, W. S. Chae, G. R. Yi and B. J. Kim, *Small*, 2013, **9**, 2667–2672.
- 7 Z. Lu, G. Liu, H. Phillips, J. M. Hill, J. Chang and R. A. Kydd, *Nano Lett.*, 2001, **1**, 683–687.
- 8 P. Chi, Z. Wang, B. Li and A.-C. Shi, *Langmuir*, 2011, **27**, 11683–11689.
- 9 R. Deng, F. Liang, W. Li, S. Liu, R. Liang, M. Cai, Z. Yang and J. Zhu, *Small*, 2013, **9**, 4099–4103.
- 10 Z. Jin and H. Fan, *Soft Matter*, 2014, **10**, 9212–9219.
- 11 A.-C. Shi and B. Li, *Soft Matter*, 2013, **9**, 1398–1413.
- 12 J. Xu, K. Wang, J. Li, H. Zhou, X. Xie and J. Zhu, *Macromolecules*, 2015, **48**, 2628–2636.
- 13 H. Yabu, K. Motoyoshi, T. Higuchi and M. Shimomura, *Phys. Chem. Chem. Phys.*, 2010, **12**, 11944–11947.

- 14 J. M. Shin, M. P. Kim, H. Yang, K. H. Ku, S. G. Jang, K. H. Youm, G.-R. Yi and B. J. Kim, *Chem. Mater.*, 2015, **27**, 6314–6321.
- 15 R. Deng, S. Liu, J. Li, Y. Liao, J. Tao and J. Zhu, *Adv. Mater.*, 2012, **24**, 1889–1893.
- 16 J. Xu, K. Wang, R. Liang, Y. Yang, H. Zhou, X. Xie and J. Zhu, *Langmuir*, 2015, **31**, 12354–12361.
- 17 D. Klinger, C. X. Wang, L. A. Connal, D. J. Audus, S. G. Jang, S. Kraemer, K. L. Killops, G. H. Fredrickson, E. J. Kramer and C. J. Hawker, *Angew. Chem., Int. Ed.*, 2014, **53**, 7018–7022.
- 18 R. Deng, F. Liang, W. Li, Z. Yang and J. Zhu, *Macromolecules*, 2013, **46**, 7012–7017.
- 19 B. V. K. J. Schmidt, J. Elbert, D. Scheid, C. J. Hawker, D. Klinger and M. Gallei, *ACS Macro Lett.*, 2015, **4**, 731–735.
- 20 S.-J. Jeon, G.-R. Yi and S.-M. Yang, *Adv. Mater.*, 2008, **20**, 4103–4108.
- 21 K. H. Ku, H. Yang, S. G. Jang, J. Bang and B. J. Kim, *J. Polym. Sci. Polym. Chem.*, 2016, **54**, 228–237.
- 22 K. H. Ku, H. Yang, J. M. Shin and B. J. Kim, *J. Polym. Sci. Polym. Chem.*, 2015, **53**, 188–192.
- 23 S. G. Jang, D. J. Audus, D. Klinger, D. V. Krogstad, B. J. Kim, A. Cameron, S.-W. Kim, K. T. Delaney, S.-M. Hur, K. L. Killops, G. H. Fredrickson, E. J. Kramer and C. J. Hawker, *J. Am. Chem. Soc.*, 2013, **135**, 6649–6657.
- 24 K. H. Ku, J. M. Shin, M. P. Kim, C.-H. Lee, M.-K. Seo, G.-R. Yi, S. G. Jang and B. J. Kim, *J. Am. Chem. Soc.*, 2014, **136**, 9982–9989.
- 25 J. A. Champion and S. Mitragotri, *Proc. Natl. Acad. Sci. U.S.A.*, 2006, **103**, 4930–4934.
- 26 H. Yang, K. H. Ku, J. M. Shin, J. Lee, C. H. Park, H.-H. Cho, S. G. Jang and B. J. Kim, *Chem. Mater.*, 2016, **28**, 830–837.
- 27 A. W. Bosse, C. J. Garcia-Cervera and G. H. Fredrickson, *Macromolecules*, 2007, **40**, 9570–9581.
- 28 L. Li, K. Matsunaga, J. Zhu, T. Higuchi, H. Yabu, M. Shimomura, H. Jinnai, R. C. Hayward and T. P. Russell, *Macromolecules*, 2010, **43**, 7807–7812.
- 29 S. Mei and Z. Jin, *Small*, 2013, **9**, 322–329.
- 30 H. Yu, X. Qiu, N. Moreno, Z. Ma, V. M. Calo, S. P. Nunes and K.-V. Peinemann, *Angew. Chem., Int. Ed.*, 2015, **54**, 13937–13941.
- 31 H. Yu, X. Qiu, S. P. Nunes and K.-V. Peinemann, *Angew. Chem., Int. Ed.*, 2014, **53**, 10072–10076.
- 32 Y. Wang, U. Goesele and M. Steinhart, *Nano Lett.*, 2008, **8**, 3548–3553.
- 33 Y. Wang and F. B. Li, *Adv. Mater.*, 2011, **23**, 2134–2148.
- 34 Y. Ruan, L. Gao, D. Yao, K. Zhang, B. Zhang, Y. Chen and C.-Y. Liu, *ACS Macro Lett.*, 2015, **4**, 1067–1071.
- 35 J. Xu, Y. Wu, K. Wang, L. Shen, X. Xie and J. Zhu, *Soft Matter*, 2016, **12**, 3683–3687.
- 36 J. Ruokolainen, R. Mäkinen, M. Torkkeli, T. Mäkelä, R. Serimaa, G. ten Brinke and O. Ikkala, *Science*, 1998, **280**, 557–560.